https://doi.org/10.1051/e3sconf/202567203013

Capacity of a cooling system with active chilled beams at different air flow rates

Jevgeni Lukaštšuk[1*], *Alo* Mikola[1,2], *Jarek* Kurnitski[1,2], *Martin* Thalfeldt[1], and *Panu* Mustakallio[3,4]

[1] Department of Civil Engineering and Architecture, Tallinn University of Technology, Tallinn, Estonia
[2] Department of Civil Engineering, Aalto University, Espoo, Finland
[3] Department of Mechanical Engineering, Aalto University, Espoo, Finland
[4] Halton Oy, Kausala, Finland

Abstract. The accuracy of dimensioning heating, ventilation and air conditioning systems (HVAC) becomes very important in the designing and construction of nearly-zero energy building (NZEBs). Over-dimensioned HVAC systems on one hand are an investment issue or on cost-effectiveness of construction works for achieving the required energy efficiency demands. On the other hand, the HVAC systems' performance might not be optimal, especially at low heating and cooling needs. For analysing and optimizing the performance of HVAC systems during such conditions and outside working hours, detailed data about the heating and cooling room units is necessary. Cooling capacity of active chilled beams under design conditions as well as at zero airflows is an input parameter in simulation tools. Real cooling capacities of active chilled beams at lower than design and at zero air flows are largely unknown, but this data is also required for thermal comfort modelling and indoor climate systems optimal sizing in buildings with active chilled beams, where the building may overheat outside the occupied hours or to optimize the schedule of ventilation systems. The aim of this study is to map the performance of active chilled beams under varying control regimes of AHU fans. The cooling capacity of active chilled beams was measured in laboratory conditions at different air flow rates including zero air flows, when air handling units (AHU) are turned off. According to measurements, the cooling capacity of active chilled beams at zero air flows reduced to ~9% of calculated capacities at design conditions. The measurement results of the current work can be used in building simulations with active chilled beam systems for indoor thermal comfort, HVAC systems optimal sizing and operations.

1. Introduction

1.1 Active chilled beams

Energy efficient technologies for indoor climate systems in buildings are assumed to play a very important role in switching to sustainable societies. However, while the demand for space heating in the EU and the OECD countries is not expected to grow any further, the demand for space cooling is expected to rise substantially [1]. The growing demand is caused by climate change, increased thermal comfort requirements and by more insulated building envelopes in cold regions. A good option of energy efficient technology for space cooling is the use of active chilled beams (ACBs) for favourable performance regarding energy efficiency, thermal comfort, and economy. A key opportunity with ACBs is utilization of high-temperature cooling. This provides major benefits such as increased use of free cooling, efficient operation of chillers, reduced latent load, reduced risk of condensation and reduced thermal losses in the chilled water distribution system [2]. Several ACB types have been produced during the last decades. However, the operation of different type of ACBs in general is the common. Pre-cooled primary air is provided from an air handling unit (AHU) while chilled water is circulated through a cooling coil inside the ACB. Primary air enters the room via a static pressure chamber and nozzles along the beam above the coil. The high primary air velocity generated by the nozzles induces secondary air (room air) that cools down when it passes the coil. The mixed air is then discharged into the room through slots along both long (or all four) sides of the beam. The secondary air flow rate divided by the primary air flow rate is referred to as the induction ratio. The flow of chilled water is usually controlled according to the room air temperature and the setpoint in order to to match the cooling capacity with the actual demand with a room thermostat.

In general, ACB cooling capacity consists of two components: pre-cooled primary air and cooling coil capacity (water side), which largely depends on the secondary air flow induced by the primary air. In this sense, the efficiency of the ACB system directly depends on the operation of the AHU. Due to the attempts to optimize the energy costs of the building's technical systems (a large part of which falls on the

* Corresponding author:jevgeni.lukastsuk@taltech.ee

ventilation system), work schedules full rotation speeds of the fans are often implemented in ventilation systems. Situations arise, when the ACBs systems work at lower or no primary air flow, i.e. at reduced secondary air flow rate. Since in general ACB manufacturers do not publish the efficiency of ACBs at lower air flows and static pressure, there is uncertainty when designing ACB systems, what is the actual cooling effect of ACBs at low AHU speed. When simulating cooling loads the efficiency of ACB-s is often not considered at all, when AHUs are out of full operation.

The current work was aimed to experimentally evaluate and analyse ACBs efficiency at different primary airflow rates with the main focus on the low primary air flow and static pressure conditions.

2. Methods

Two different ACB types from two different producers were tested in the Tallinn University of Technology Air Distribution Lab: ACB-1 and ACB-2.
ACB-1 is a linear type of beam with mixed air discharging into the room through slots along two long sides of the beam. ACB-2 mixed air discharging through four sides of the beam. Both beams are designed for suspended ceiling installation and have the same length and width, 1200 x 600mm. While ACBs construction and coils sizes are different an efficiency of the tested objects can differ respectively.
The study was conducted in the following steps:

1. Measurements of the cooling capacity of ACBs cooling circuits at different primary air flow rate with relatively constant water flow rates and room temperatures.
2. Assessment of the share of cooling capacity from the ACBs cooling coils and the connected water pipes.
3. Comparison of the results with the selection software output of the respective ACBs.
4. Recommendations for simulating cooling systems with ACBs and schedule-based control of AHUs.

2.1 Experimental setup

ACB-1 and ACB-2 were tested in a 46.1 m2 test room - 8.7m long and 5.3m wide. The height of the test-room under a suspended ceiling is 3.0m. Both ACBs were installed at the bottom surface height 2.8 m from the floor under the suspended ceiling. The experimental setup is presented in figure Fig. 1. Primary air was provided by separate AHU, which serves the lab only. For primary air connections uninsulated round ducts DN125 with air flow control damper (IRIS) were used, equipped with air-pressure drop measurement connections. Primary air temperature set-point was 16°C for all the measurements. For water side connections uninsulated composite plastic pipes De16x2.0 6 were used. Chilled water was provided by a centralized cooling system, which was operated during experiments with supply temperature set-point 15˚C. ACB loop circulation pump operated at constant differential pressure mode. ACB-1 and ACB-2 were tested one at a time and on separate days, but the same control algorithms were used for both beams.
Six electrical radiators (EHR) with 1000W capacity were installed in the perimeter and controlled to maintain 25…26˚C in the room [3]. The room had internal constructions only, which were not thermally insulated from surrounding spaces. The room air temperature of at least 22.5 ˚C was ensured in surrounding spaces to reduce their impact on the measurements.

ACB-1 and ACB-2 were tested at primary air flow rates in the following sequence: 0 l/s →20 l/s (22 l/s for ACB-2) →15 l/s →10 l/s →5 l/s. The primary air flow was controlled by changing the speed of AHU fans. ACB-1 and ACB-2 were tested at constant water flow rate of ~0.053 kg/s by using a constant differential pressure valve AB-QM 4 DN15 [4]. The cooling meter Kamstrup Multical 403 (DN15 q_{nom}0.6m^3/h) equipped with temperature sensors pair Pt500 (installed in water flow) was used for water temperatures and water-flow measurements [5]. Air temperatures at different heights and positions (see Fig. 1), water temperatures and the water flow data were logged during 30 minutes with sample intervals of 30 seconds for every primary air flow rate respectively. USB M-bus converter with respective software was used for cooling meter data logging and gathering. The performance of ACB was also inspected with a smoke test and a thermal camera.

The main used measurement equipment`s specification is presented in Table 1.

Table 1. Specifications of measuring equipment.

	HOBO UX120-006M TMC6-HD / TMC6-HE	**KAMSTRUP MULTICAL 403 q_{nom}=0.6m3/h, Class2 (E1, M2)**	**Temperature sensors pair Pt500**	**Testo 440 dP**
Parameters	air temperature	water flow	water temperature	differential air pressure
Range	-40…100 °C	0.006…1.2 m^3/h	2…180 °C	-150 to +150 hPa
Accuracy	± 0.15 °C	(*see in section 2.2.1*)	(*see in section 2.2.1*)	<100 Pa ±0.05 Pa

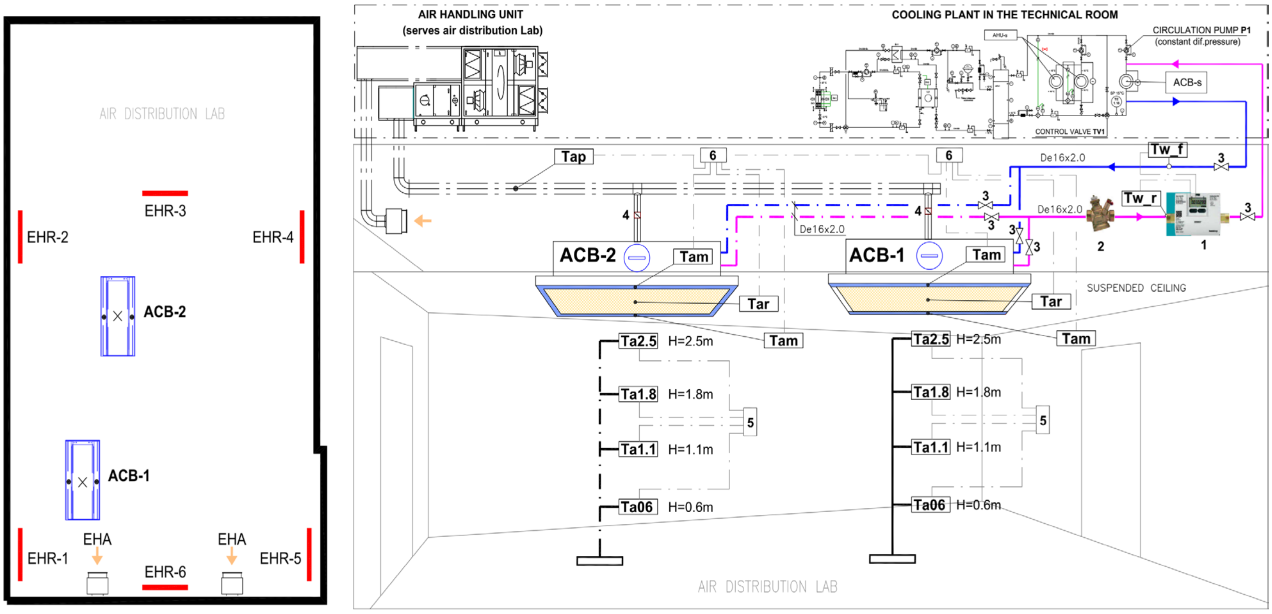

(1) (2)

Measurement setup:
(1) Test-room layout: X and • measurement points, EHR -electric heating radiator (1000W), EHA – exhaust air;
(2) Schematic of the test-room and control system: *1* - cooling meter Kamstrup Multical 403 Qnom=60 l/h, *2* -constant differential pressure valve AB-QM DN15, *3* - shut-off valve, *4* - air-flow control damper IRIS, *5* and *6* - data logger Onset HOBO UX120-006M; T_a0.6..2.5 - air temperature measured at height from the floor H=0.6...2.5m (°C), T_{ar} - reference air temperature (°C), T_{am} – ACB leaving mixed air temperature (°C) , T_{ap} – primary air temperature(°C).

2.2 Calculations

2.2.1 Calculation of water temperature increase.

Owing to the fact that ACB`s chilled water pipe connections were not thermally insulated during the measurements, the impact of heat losses of the pipes was calculated separately for supply Δt_{ws} and return Δt_{wr} temperatures for every measurement using Equations 1, 2, 3.

$$\Delta t_{ws} = t_o - t_{ws} \quad ,(°C) \tag{1}$$

$$t_o = t_{ws} - \frac{\gamma \cdot l}{(q \cdot c_w)} \quad ,(°C) \tag{2}$$

$$\gamma = \frac{\pi \cdot (T_a 2.8 - t_{ws})}{0.5 \cdot \lambda \cdot ln\frac{d_e}{d_i} + \frac{1}{d_e \cdot \alpha_v}} \quad ,(W/K) \tag{3}$$

Thermal conductivity of pipe material λ=0.4 W/m·K [6] was used in the calculations. In cooling capacity calculations Δt_{w_f} was added to measured supply water temperature and Δt_{w_r} was subtracted from measured return water temperature as well.

2.2.2 Calculation of measurement uncertainties

Accuracy of measured water temperature and water-flow was major for cooling capacity calculations in this study. Uncertainties for water temperatures E_{tw} and water flow E_{qw} were calculated in accordance with the cooling meter's technical sheet recommendations 5 for every measurement separately using Equations 4, 5, 6. The total length (*l*) of uninsulated pipe from the water sensors to the ACB connection of 2.8m (inlet or return) and 5.1m (inlet or return) was taken in calculations for ACB-1 and ACB-2 respectively.

$$E_{tot} = E_{tw} + E_{qw} \quad ,(\%) \tag{4}$$

$$E_{tw} = \pm\left(0.4 + \frac{4}{\Delta t_w}\right) \quad ,(\%) \tag{5}$$

$$E_{qw} = \pm\left(1 + 0.01 \cdot \frac{q_{nom}}{q}\right) \quad ,(\%) \tag{6}$$

2.1.1 Calculation of cooling capacities

ACB cooling capacity was calculated on the base of measured parameters. For calculations, Equations 7, 8, 9, 10, 11, 12 were used.

$$P_{tot} = P_w + P_a \quad ,(W) \tag{7}$$

$$P_w = q \cdot (t_{ws} - t_{wr}) \cdot c_w \quad ,(W) \tag{8}$$

$$P_{w\_min} = q \cdot (t_{wr} - t_{ws}) \cdot c_w \cdot \left(1 - \frac{E_{tot}}{100}\right) ,(W) \tag{9}$$

$$P_{w\_max} = q \cdot (t_{wr} - t_{ws}) \cdot c_w \cdot \left(1 + \frac{E_{tot}}{100}\right) ,(W) \tag{10}$$

$$P_a = Q_a \cdot (T_{ar} - T_{ap}) \cdot c_a \cdot \rho_a \quad ,(W) \tag{11}$$

$$P_p = q \cdot (\Delta t_{ws} + \Delta t_{wr}) \cdot c_w \quad ,(W) \tag{12}$$

2.3 Temperature sensor calibration

Before performing the measurements, the cooling meter's water sensors pair Pt500 was calibrated by measuring water temperature in the water tank for 10 minutes with sample logging interval of 10 seconds. After measurement the mean water temperature difference was 0.0116°C divided by sensors pair.

3. Results

3.1 Pre - measurement calculations

Water temperature increase, influenced by heat-losses from uninsulated pipes, was calculated in accordance with the description in section 2.2.1. The results presented in figure Fig. 2 were taken for further cooling capacity calculations. At low primary air-flow rates water temperature increase in the pipes was significant relatively to temperature increase in the ACB`s coil.

Calculated uncertainties for measured water temperatures E_{tw} and water-flow E_{qw} are presented in figure Fig. 3. Uncertainty of water temperatures was greater at zero and 5 l/s primary air flow rates due to lower water temperature difference under those conditions and was significant for calculations of cooling capacities for both ACB-1 and ACB-2. Uncertainty of water flow was the same for all measurement conditions and did not have a large impact on further calculations. Calculated values E_{tw} and E_{qw} were taken in further calculations of cooling capacities in accordance with the description in section 2.2.3.

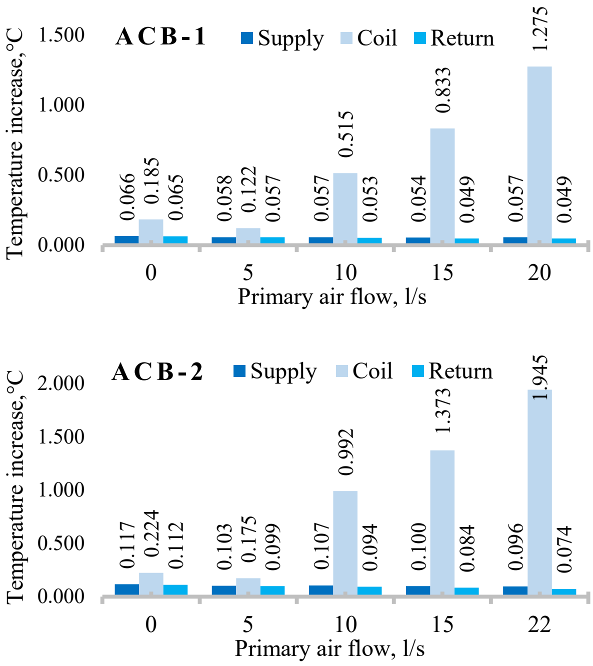

Water temperature increase in the system.

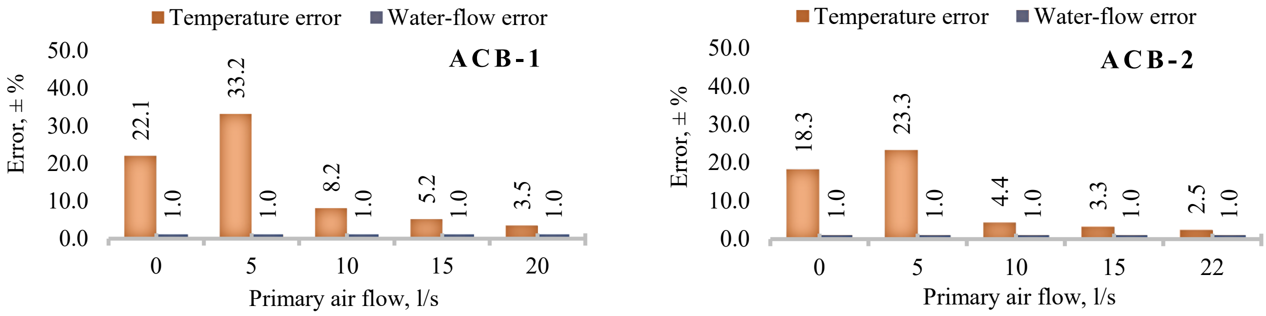

Measurement uncertainties for measured water temperatures E_{tw} and water-flow E_{qw} .

3.2 ACB-1 measurement results

ACB-1 measured chilled water temperatures, air temperatures and water-flow values after calculations in accordance with the descriptions in section 2.2 are presented in figure Fig. 4.

Supply water temperature and water-flow were relatively constant during the experiments at different air-flow rates. The rise of return water temperature and the rise of mean water temperature t_{w_m} depending on the rise of primary air-flow rate and the static air pressure characterizes mainly an efficiency of ACB's cooling coil due to increased induction ratio of secondary air. For the same reason ACB discharging mixed air temperature T_{am} was lower than the reference air temperature T_{ar} and their difference was rising due to the rise of primary air static pressure. The fact that the mixed air temperature T_{am} was higher than the reference air temperature T_{ar} at a primary air-flow rate of 0 l/s refers to the hypothesis, that ACB secondary air movement over the coil was in a down-flow direction, occurred purely by natural convection. That hypothesis was proven by a smoke test and can also be evaluated in figure Fig. 6. Higher primary air temperature T_{ap} at lower primary air-flow rates was cased by heat-losses through the supply air duct due to lower air velocity in the ducts.

ACB-1 cooling capacities at different primary air-flow and static air pressure rates are presented for water side P_w and as total capacity P_{tot} in figure Fig. 5. Water side P_{w_min} and P_{w_max} values are also presented to indicate uncertainties. The results of software calculations have been added for comparison. Due to the fact that ACB-2 software does not allow to size under low primary air either static air pressure rate conditions Pa_stat under 40Pa, only at design conditions (primary air-flow 20 l/s and static air pressure 70Pa) software results were added to figure Fig. 5.

 https://doi.org/10.1051/e3sconf/202567203013

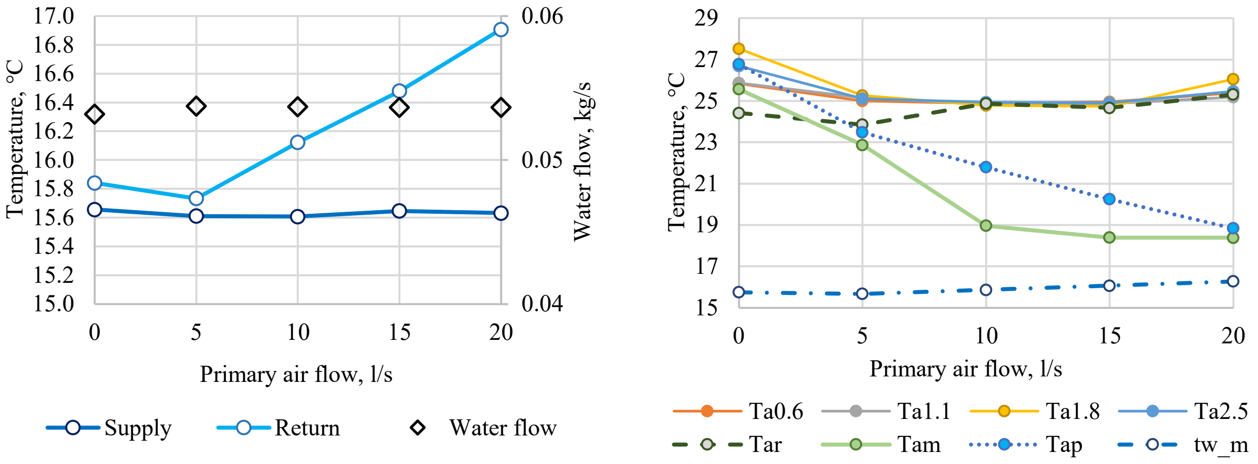

(1) (2)

ACB-1 measurement results: (1) measured water temperatures, (2) measured air temperatures and mean water temperature.

Under design conditions the value $P_w - SW$ 314W exceeded the measured value P_w 283W by 9.9% and P_{w_max} 296W by 5.7% respectively. And under the same conditions $P_{tot} - SW$ 462W exceeded the measured value P_{tot} 439W by 5%. At zero primary air-flow rate the measured value P_{tot} was 38W. The ratio P_{tot} at zero primary air-flow to P_{tot} at design conditions was 8.8%. Decrease of ACB`s cooling capacity at a reduced primary air-flow and the static air pressure rate was due to a reduced induction ratio of secondary air. Measured cooling capacity at primary air-flow rate 5 l/s was lower than at a zero air-flow rate. The ceiling integrated ACB model was tested under the suspended ceiling. The air distribution could affect the cooling capacity measurement due to possible short-circuit from the air jet leaving beam to induction air (not enough surface for Coanda effect). For the same reason, the measured results could differ from software results.

It should also be noted that the reference air temperature was lower than the mixing air temperatures at zero air-flow rate due to the secondary air movement over the coil in a down-flow direction. At zero primary air-flow rate T_{am} should be taken as reference air temperature for cooling capacity calculations. Thus, the difference of reference air and mean water temperatures was greater at zero primary air flow than under 5 l/s primary air conditions.

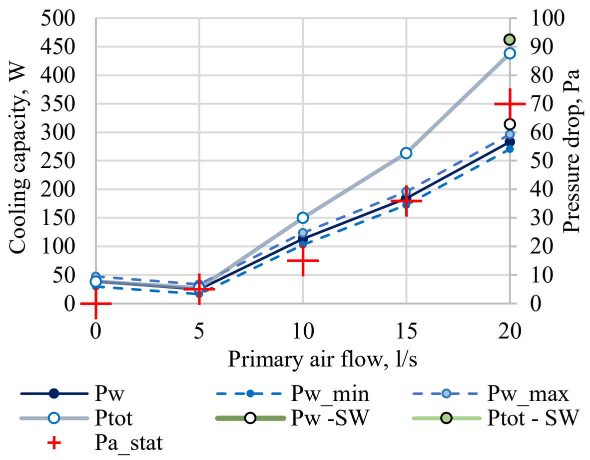

ACB-1 cooling capacities at a different airflow rate.

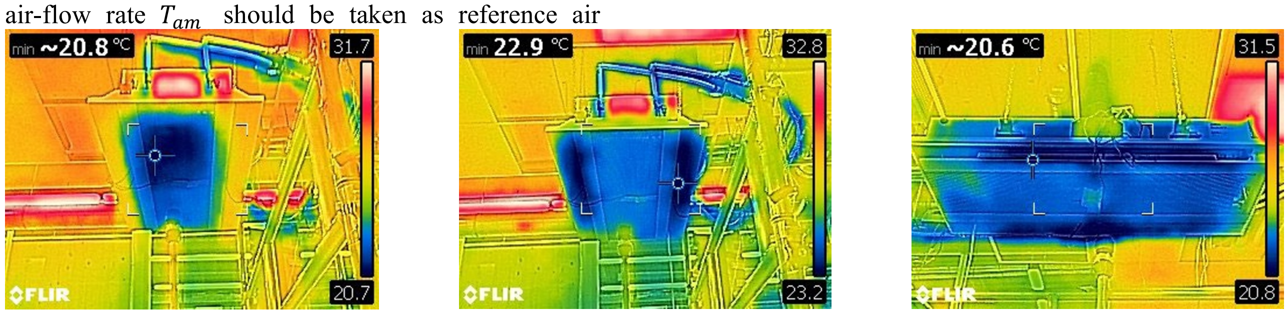

(1) (2) (3)

ACB-1 cooled air flow at different primary airflow rates: (1) air flow 0 l/s, (2) air flow 10 l/s, (3) air flow 20 l/s.

3.3 ACB-2 measurement results

ACB-2 measured chilled water temperatures, air temperatures and water-flow values after calculations in accordance with descriptions in section 2.2, are presented in figure Fig. 7.

Despite the fact that ACB-1 and ACB-2 have different designs and were tested at different times, their measurement results were overall similar.

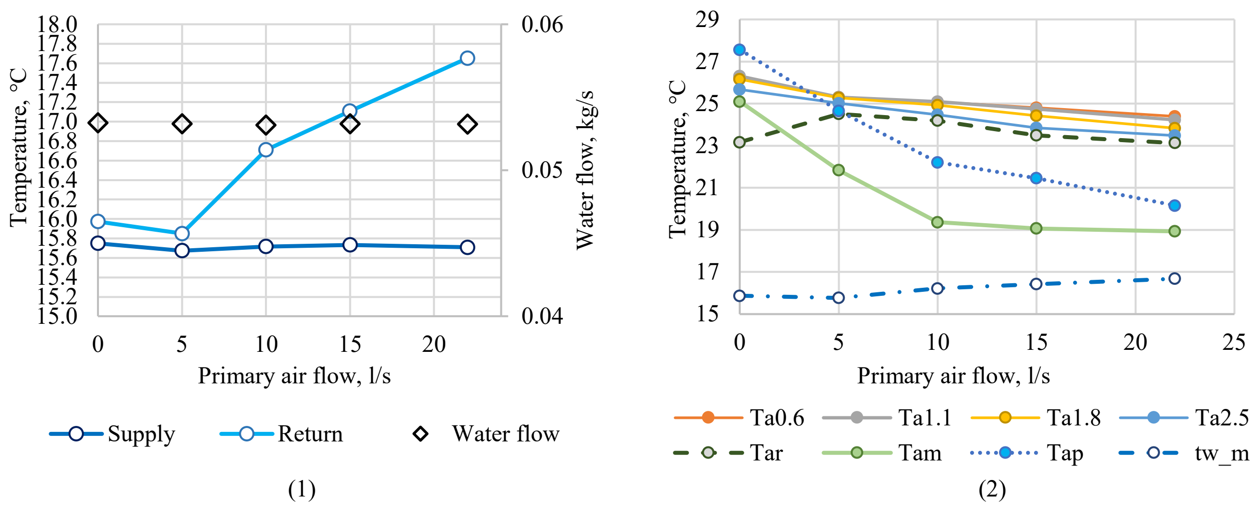

ACB-2 measurement results: (1) measured water temperatures, (2) measured air temperatures and mean water temperature.

Supply water temperature and water-flow were relatively constant during the experiments at different air-flow rates. The rise of return water temperature and the rise of mean water temperature t_{w_m} depending on the rise of primary air-flow rate and the static air pressure characterizes mainly an efficiency of ACB`s cooling coil due to increased induction ratio of secondary air. For the same reason ACB discharging mixed air temperature T_{am} was lower than reference air temperature T_{ar} and their difference was rising due to the rise of primary air static pressure. The fact that mixed air temperature T_{am} was higher than reference air temperature T_{ar} at primary air-flow rate 0 l/s refers to hypothesis that ACB secondary air movement over the coil was in a down-flow direction, occurred purely by natural convection. That hypothesis was proven by a smoke test and can also be evaluated in Fig. 9. Higher primary air temperature T_{ap} at lower primary air-flow rates was cased by heat-losses through the supply air duct due to lower air velocity in the ducts.

ACB-2 cooling capacities at different primary air-flow and static air pressure rates are presented for water side P_w and as total capacity P_{tot} in figure Fig. 8. Water side P_{w_min} and P_{w_max} values are also presented to indicate uncertainties. The results of software calculations have been added for comparison. Due to the fact that ACB-2 software allows to size at static air pressure rate at least 30 Pa, only corresponding software results were added to figure Fig. 8. ACB-2 data of natural convection cooling capacity at zero primary air flow have also been presented in figure Fig. 8.

Under design conditions (primary air-flow rate 22 l/s Pa_stat =70Pa) the value $P_w - SW$ 480W exceeds the measured value P_w 430W by 10.4% and P_{w_max} =445W by 7.3% respectively. And under the same conditions $P_{tot} - SW$ 556W exceed the measured value P_{tot} 508W by 8.6%. In comparison of the results at zero primary air-flow rate $P_{tot} - SW$ 42W differs from the measured value P_{tot} 47W by 11.9%. The ratio P_{tot} at zero primary air flow to P_{tot} at design conditions is 9.3% for measured values and 7.6% for software values. Decrease of ACB`s cooling capacity at reduced primary air-flow and the static air pressure rate was due to reduced induction ratio of secondary air as well. Measured cooling capacity at primary air-flow rate 5 l/s was lower, than at zero air-flow rate. The ceiling integrated ACB model was tested under the suspended ceiling. The air distribution could affect the cooling capacity measurement due to possible short-circuit from the air jet leaving beam to induction air (not enough surface for Coanda effect). For the same reason, the measured results could differ from software results.

It should also be noted that the reference air temperature was lower than the mixing air temperatures at zero air-flow rate due to the secondary air movement over the coil in a down-flow direction. At zero primary air flow-rate T_{am} should be taken as reference air temperature for cooling capacity calculations. Thus, the difference of reference air and mean water temperatures was greater than under 5 l/s primary air conditions.

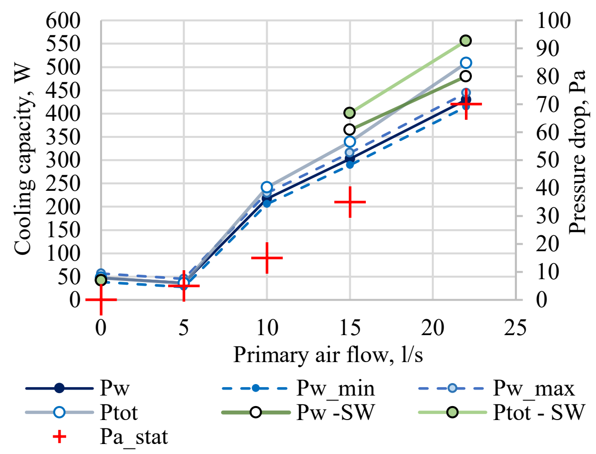

ACB-2 cooling capacities at different air flow rate.

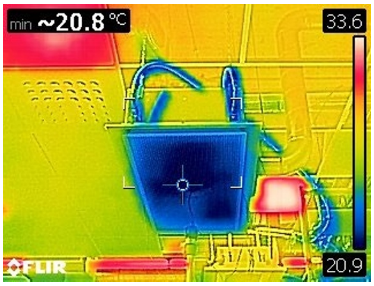

(1)

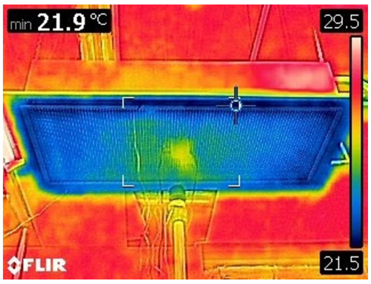

(2)

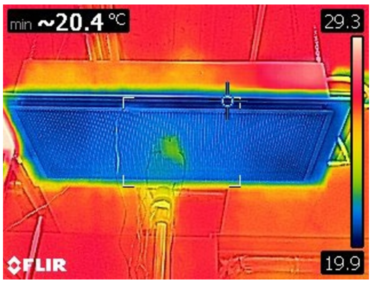

(3)

ACB-2 cooled air flow at different primary air-flow rates: (1) air flow 0 l/s, (2) air flow 10 l/s, (3) air flow 22 l/s.

3.4 Summary of ACB-1 and ACB-2 measurement results

ACB-1 and ACB-2 cooling capacity fractions in comparison with calculated heat losses from uninsulated connection pipes (as a part of the systems) are presented in figure Fig. 10.

At low primary air-flow rates the pipes heat losses constitute significant part of the cooling energy delivered to the served space. Under zero air-flow rate conditions the heat gain transferred to the pipes was almost the same as ACB`s cooling capacity. In both cases the cooling capacity at zero primary air-flow was grater that at 5 l/s. That could be caused by affected air-jet at low primary air-flow rates. The ceiling integrated ACB model was tested under a suspended ceiling, air distribution could affect the cooling capacity measurement due to possible short-circuit from air jet leaving beam to induction air (not enough surface for Coanda effect).

ACB-1 and ACB-2 cooling capacity ratio at different primary air-flow rates to ACB's cooling capacity under design conditions is presented in figure Fig. 11.

The curve *ACB + pipes* describes the cooling capacities ratio with uninsulated connection pipes heat losses included. In both cases *ACB + pipes* ratio at zero air-flow was significant. When using a plastic composite pipe, the heat losses constitute 6.6% and 10% of ACB design efficiency for the "short" and for the "long" connections respectively. And the system's (*ACB + pipe*) cooling efficiency ratio is ~15% and ~19% for the "short" and for the "long" connections respectively. For this reason, the potential of ACB systems (ACB + pipe) convection cooling mainly at zero air-flow rates should be researched in further works as a pre-cooling option in schedule operated AHU systems for cooling loads reduce.

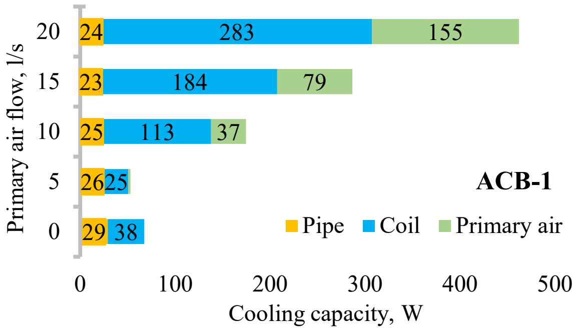

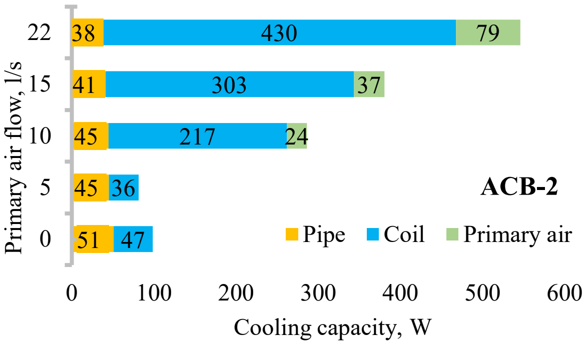

Cooling capacity fractions at different primary air-flow rates.

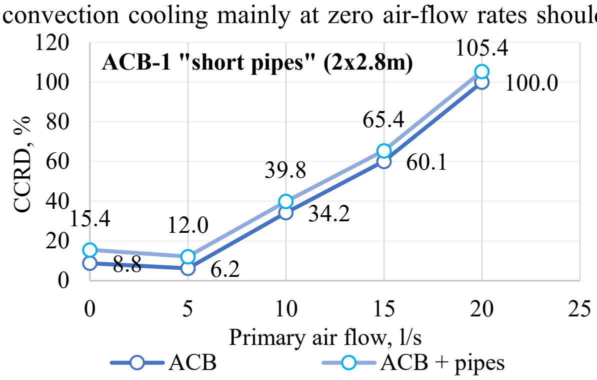

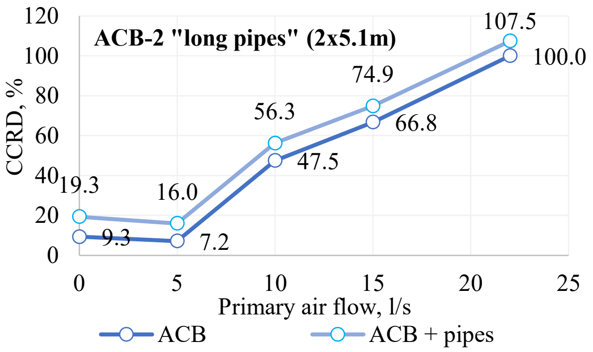

Ratio of cooling capacity to ACB cooling capacity at design air-flow rate (CCRD).

4. Discussion

This experimental work was mainly aimed to evaluate the efficiency of ACBs at low primary air-flow rates, when AHU is operated under reduced air-flow conditions either stopped for unoccupied hours. This experimental work was performed in contact with Halton Oy specialists, who have tested an analogue beam to ACB-1 in the Halton Oy Lab. Halton Oy measurement conditions differed from current working conditions mainly due to used methodologies for passive chilled beams cooling capacity measurements. However, the results under the same conditions were quite similar. In this context the current works measurement results could be evaluated as accurate enough for concluding.

According to results of the current work, there is a potential of ACBs systems to reduce cooling loads by pre-cooling during unoccupied hours, in schedule operated AHU systems. The first option is to keep a low room temperature set-point in zones during unoccupied hours and especially at nighttime for free-cooling utilization. Zone cooling control valves will provide required water-flow to ACBs and natural convection cooling potential can be utilized with mainly circulation pump energy use. Another option, additionally to the previous one, is to design ACBs systems with uninsulated zone pipework. Of course, that is a controversial idea. It is typically recommended to insulate all chilled water pipes as much as possible (especially supply water pipe) to provide designed water temperature and ACB cooling capacity to cooled space, but that concerns mainly to AHU operated conditions. It would be useful to evaluate the impact of uninsulated pipes to the cooled spaces in the complex. If uninsulated connection pipes impact the total cooling capacity (ACB + pipes) provided to zones is not significant at AHU operated hours, there is an option for increasing natural convection cooling potential, when schedule operated AHU is stopped. Additionally, the impact of uninsulated pipe heat losses with different materials can be researched in more detail. For instance, in visible ACB pipes installations there is a very common thin-wall (1.2mm) galvanized steel-press pipework, which has a thermal conductivity λ =58 W/m · K, and in this case the impact of uninsulated pipes should be greater. Of course, the impact of the uninsulated pipework to a cooled space depends on the suspended ceiling design. In that sense it would be very useful to research this issue in further works in details at different situations and in the complex.

Conclusion

Based on performed measurement results it can be concluded the following:

1. ACB-1 and ACB-2 cooling efficiency ratio at zero air-flow to design capacity is ~9.0%, provided purely by natural convection.
2. When uninsulated connection pipes installations are used, the pipework`s heat loss constitutes a significant part of cooling energy at zero primary air-flow provided to the served space. In case of a plastic composite pipe, the heat losses constitute 6.6% and 10% of ACB design efficiency for the “short” and for the “long” connections respectively. And the system`s (*ACB + pipe*) cooling efficiency ratio is ~15% and ~19% for the “short” and for the “long” connections respectively.
3. The potential of ACB systems (ACB + pipe) convection cooling mainly at zero primary air-flow rate could and should be utilized as much as possible in cooling loads calculations as the pre-cooling method to reserve thermal mass, and in that way to reduce cooling peak loads.

Acknowledgements
This work has been supported by the European Commission through LIFE IP BUILDEST (LIFE20 IPC/EE/000010), the European Union’s Horizon Europe research and innovation programme under the grant agreement No. 101057497, by the Estonian Research Council through the grants PSG409, PRG483 and PRG658.

References

1. P. Filipsson, A. Trüschel, J. Gräslund, J.-O. Dalenbäck, *A Thermal Model of an Active Chilled Beam*. Energy and Buildings, **149**, 83–90 (2017)
2. P. Filipsson, A. Trüschel, J. Gräslund, J.-O. Dalenbäck, *Modelling of rooms with active chilled beams*. Journal of Building Performance Simulation, **Vol.13**, 409-418 (2020)
3. CEN, European Committee for Standardization. *EN 15116 Ventilation in Buildings – Chilled Beams – Testing and Rating of Active Chilled Beams* (2008)
4. Fact sheet “AB-QM flow checker DN 40-250 and AB-QM 4.0 DN 15-32 Verifying the flow on AB-QM valves”. Danfoss (2023)
5. Kamstrup Multical 403 data sheet (2014)
6. Uponor composite pipe systems for drinking water distribution and heating installations. Technical Information
7. P. Filipsson, A. Trüschel, J. Gräslund, J.-O. Dalenbäck, *Induction Ratio of Active Chilled Beams - Measurement Methods and Influencing Parameters*. Energy and Buildings **129**, 445–451 (2016)